

Large-scale troughs on Vesta: A signature of planetary tectonics

D. L. Buczkowski,¹ D. Y. Wyrick,² K. A. Iyer,¹ E. G. Kahn,¹ J. E. C. Scully,³ A. Nathues,⁴ R. W. Gaskell,⁵ T. Roatsch,⁶ F. Preusker,⁶ P. M. Schenk,⁷ L. Le Corre,^{4,8} V. Reddy,^{4,8} R. A. Yingst,⁵ S. Mest,⁵ D. A. Williams,⁹ W. B. Garry,⁵ O. S. Barnouin,¹ R. Jaumann,⁶ C. A. Raymond,¹⁰ and C. T. Russell³

Received 29 June 2012; revised 23 August 2012; accepted 25 August 2012; published 29 September 2012.

[1] Images of Vesta taken by the Dawn spacecraft reveal large-scale linear structural features on the surface of the asteroid. We evaluate the morphology of the Vesta structures to determine what processes caused them to form and what implications this has for the history of Vesta as a planetary body. The dimensions and shape of these features suggest that they are graben similar to those observed on terrestrial planets, not fractures or grooves such as are found on smaller asteroids. As graben, their vertical displacement versus length relationship could be evaluated to describe and interpret the evolution of the component faults. Linear structures are commonly observed on smaller asteroids and their formation has been tied to impact events. While the orientation of the large-scale Vesta structures does imply that their formation is related to the impact events that formed the Rheasilvia and Veneneia basins, their size and morphology is greatly different from impact-formed fractures on the smaller bodies. This is consistent with new analyses that suggest that Vesta is fully differentiated, with a mantle and core. We suggest that impact into a differentiated asteroid such as Vesta could result in graben, while grooves and fractures would form on undifferentiated asteroids. **Citation:** Buczkowski, D. L., et al. (2012), Large-scale troughs on Vesta: A signature of planetary tectonics, *Geophys. Res. Lett.*, 39, L18205, doi:10.1029/2012GL052959.

1. Introduction

[2] As the Dawn spacecraft [Russell and Raymond, 2011] approached Vesta in July of 2011, large-scale linear troughs encircling the asteroid became immediately evident in

Framing Camera (FC) [Sierks et al., 2011a] images (Figure 1). When the polar Survey orbit around Vesta was reached, higher resolution images of these structures were acquired and a detailed analysis could begin.

[3] To analyze these structures, we mapped them using the Small Body Mapping Tool (SBMT) [Kahn et al., 2011]. The SBMT overlays FC clear filter images on the Vesta shape model [Preusker et al., 2012a]; thus, each mapped linear structure observed in a FC image has a topographic component to the lineament. We can therefore 1) determine the dimensions (length, width and height) and 2) create topographic profiles of each structure we map. We can also utilize the topographic component of each lineament to model the fracture plane of the related structure [Buczkowski et al., 2008; Jaumann et al., 2012]. Generally, similarly oriented fracture planes indicate that the corresponding fractures share a common formation mechanism [Buczkowski et al., 2008]. We therefore can perform a fault plane analysis by determining the pole of the plane described by each individual lineament and determine if the poles cluster or are random; clustered poles indicate that the fracture planes are oriented in a comparable manner [Buczkowski et al., 2008].

2. Observations

2.1. Divalia Fossa and the Equatorial Troughs

[4] The most prominent set of large linear structures encircle Vesta roughly aligned with the equator. While most of these structures are wide troughs bounded by steep scarps, extending in a similar orientation are muted troughs, grooves and pit crater chains. Fault plane analysis suggests that the formation of the equatorial troughs was triggered by the impact event that formed Rheasilvia basin, as the poles of the planes described by their fault traces cluster on the Rheasilvia central peak [Jaumann et al., 2012].

[5] Divalia Fossa (Figure 1a), the largest of the equatorial troughs, is ~465 km long, starting at 349.2°E and extending over the prime meridian to end at 84.1°E. Its maximum width is 21.8 km, although it can be as narrow as 14.5 km. At its western end (~350°E) the structure is muted but the southern scarp is clearly higher and steeper than the northern scarp. Moving eastward, at 0° longitude the structure resembles a classic flat-floored graben with both walls having a similar slope (Figure 2a), indicating that both the northern and southern walls are fault scarps and that there was downward movement of the trough floor along both. The southern scarp is still slightly more pronounced than the northern one at this location. However, further east Divalia Fossa is expressed by relatively steep, high northern scarps and greatly subdued southern scarps. From 30°E to 60°E the Divalia

¹Johns Hopkins University Applied Physics Laboratory, Laurel, Maryland, USA.

²Southwest Research Institute, San Antonio, Texas, USA.

³Department of Earth and Space Sciences, University of California, Los Angeles, California, USA.

⁴Max Planck Institute for Solar System Research, Katlenburg-Lindau, Germany.

⁵Planetary Science Institute, Tucson, Arizona, USA.

⁶Institute of Planetary Research, DLR, Berlin, Germany.

⁷Lunar and Planetary Institute, Houston, Texas, USA.

⁸Department of Earth System Science and Policy, University of North Dakota, Grand Forks, North Dakota, USA.

⁹School of Earth and Space Exploration, Arizona State University, Tempe, Arizona, USA.

¹⁰Jet Propulsion Laboratory, California Institute of Technology, Pasadena, California, USA.

Corresponding author: D. L. Buczkowski, Johns Hopkins University Applied Physics Laboratory, 11100 Johns Hopkins Rd., Laurel, MD 20723, USA. (debra.buczkowski@jhuapl.edu)

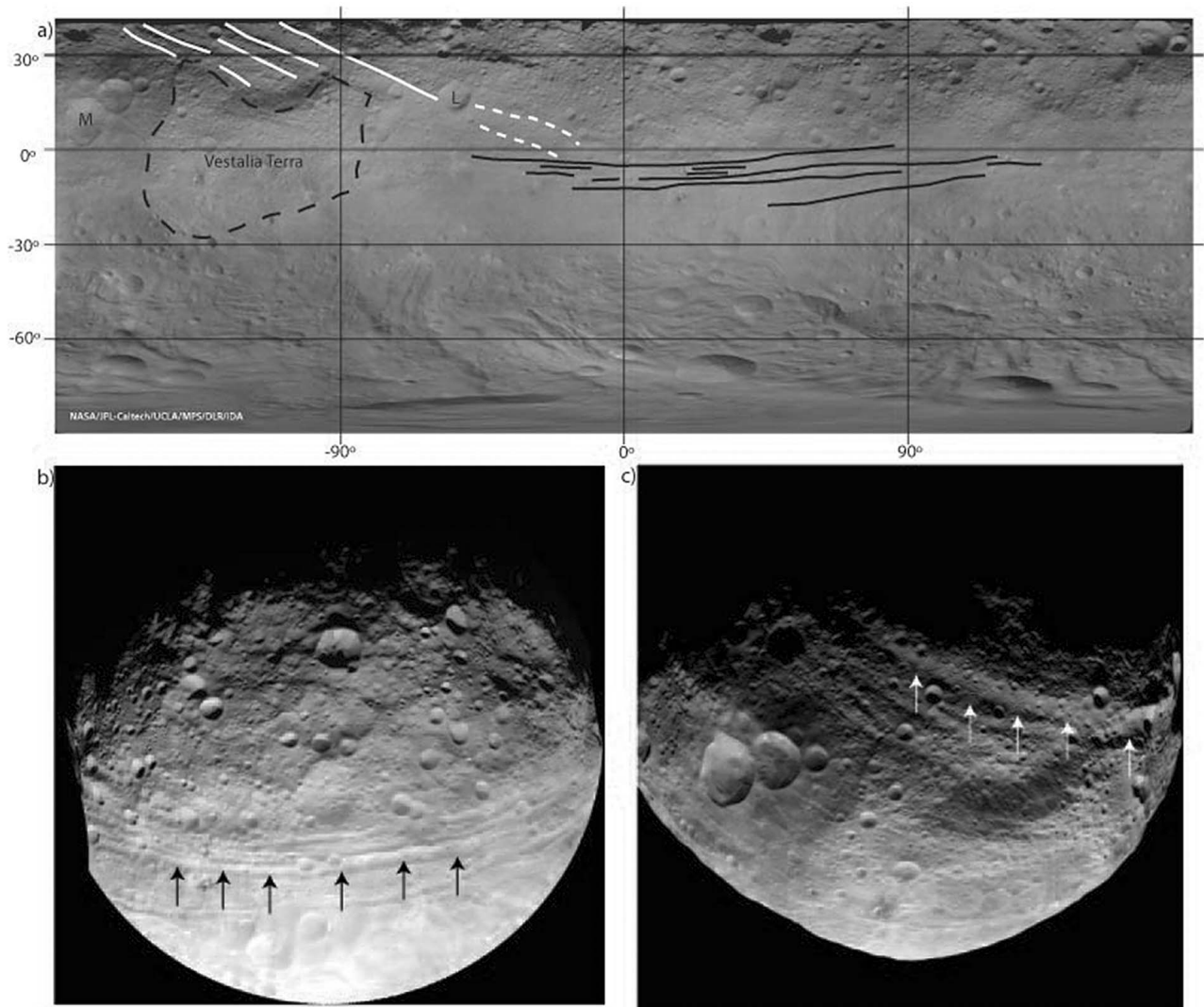


Figure 1. (a) Simple cylindrical image of Vesta shows location of giant troughs relative to each other and other features on Vesta. Black lines mark the equatorial troughs while white lines show the northern troughs; white dashed line is probable extension of Saturnalia Fossa. Black dashed line shows location of Vestalia Terra. Marcia crater and Lepida crater are labeled M and L, respectively. (b) Framing Camera clear filter images from RC3 (late approach phase) that shows equatorial troughs. Black arrows point to Divalia Fossa. (c) Clear filter FC image of Vesta showing northern troughs. White arrows point to Saturnalia Fossa.

Fossa profiles resemble half-graben [Gibbs, 1987] (Figure 2a), suggesting the northern scarp was the more active fault. By 70°E Divalia Fossa once again resembles a true graben, with both walls having a similar slope (Figure 2a), before ending at ~80°E. Analysis of the Divalia Fossa profiles indicate the graben accommodates at least 5 km of vertical displacement (Figure 2b), with the northern fault accommodating the bulk of the displacement along the fault (except from 350°E~15°E). In these analyses, we use vertical displacement (throw) as a proxy for the total displacement along each fault; the horizontal displacement component (heave) is obscured by significant post-faulting modification and thus is a less reliable measurement. Vertical displacement was measured as the highest fault elevation on each profile of each fault face minus the lowest mid-graben elevation value. All slope values are shallow relative to the dip of terrestrial extensional faults, which could suggest that these features are detachment faults

but more likely is due to extensive modification due to impact and/or mass wasting.

[6] Eighty-six additional equatorial troughs have been mapped, with lengths varying from 19–380 km and widths up to 15 km. Profiles across the suite of equatorial troughs at 55°E and 70°E longitude imply that these features are also graben and half-graben (Figure 3a). The troughs north of Divalia Fossa have a higher southern scarp, while the troughs south of Divalia have a higher northern scarp. Vertical displacement across these smaller graben is considerably less than across Divalia itself, approximately 2 km (Figure 3b).

[7] The large equatorial troughs encircle approximately 60% of Vesta, from ~313°E, west across the prime meridian, ending at ~165°E. Structures with similar orientation (per fault plane analysis [Jaumann *et al.*, 2012]) are identified in the remainder of the equatorial region. Muted troughs and grooves are found to the south of Marcia crater (Figure 1b). It

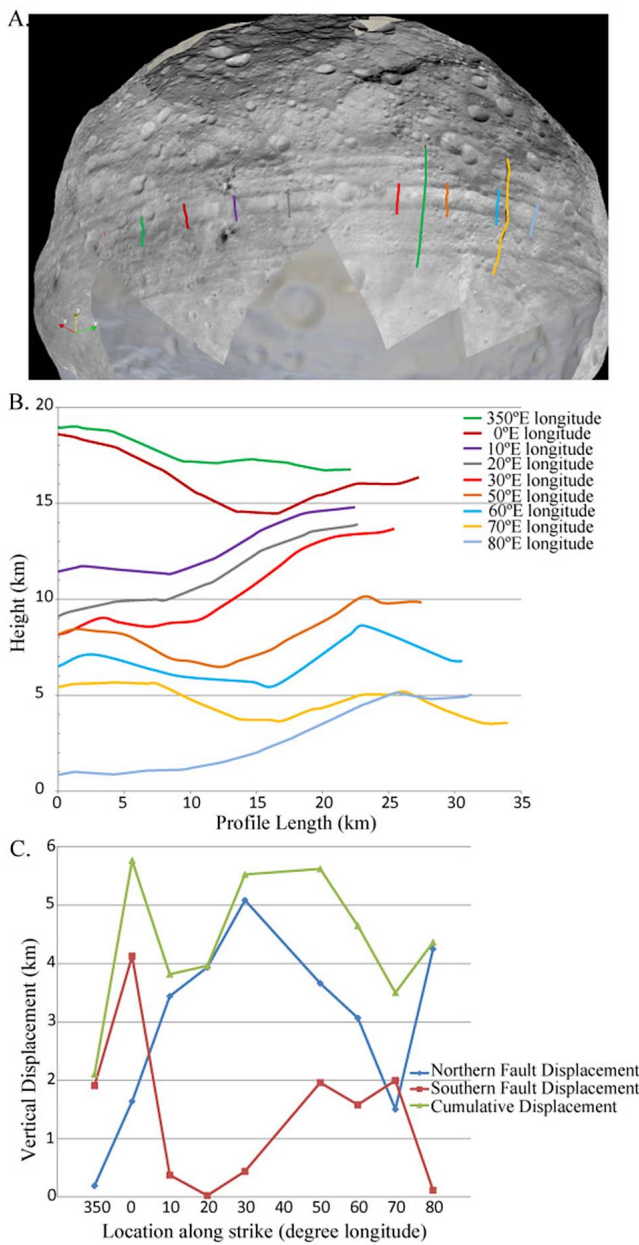


Figure 2. (a) FC images draped over the Vesta shape model in the SBMT shows location of profiles across Divalia Fossa. Short lines are Divalia Fossa profiles; longer lines represent the profiles over the suite of equatorial troughs described in Figure 3. Lines are color-coded to profiles in Figure 2b. (b) Relative topography of Divalia Fossa at 350°E, 0°E, 10°E, 20°E, 30°E, 50°E, 60°E, 70°E and 80°E longitude. Profiles go from south to north across the trough. Vertical exaggeration is $\times 2$. (c) Displacement on the northern (blue) and southern (red) faults of Divalia Fossa and cumulative displacement (green) on the graben.

is likely that ejecta from the crater covered pre-existing large equatorial troughs, muting their topographic signature in this location. No equatorial troughs cut the topographically high plateau known as Vestalia Terra (Figure 1b) but pit

crater chains with a similar orientation have been identified [Buczowski *et al.*, 2012]. We suggest that these pit crater chains are the surface representation of sub-surface faulting below the plateau.

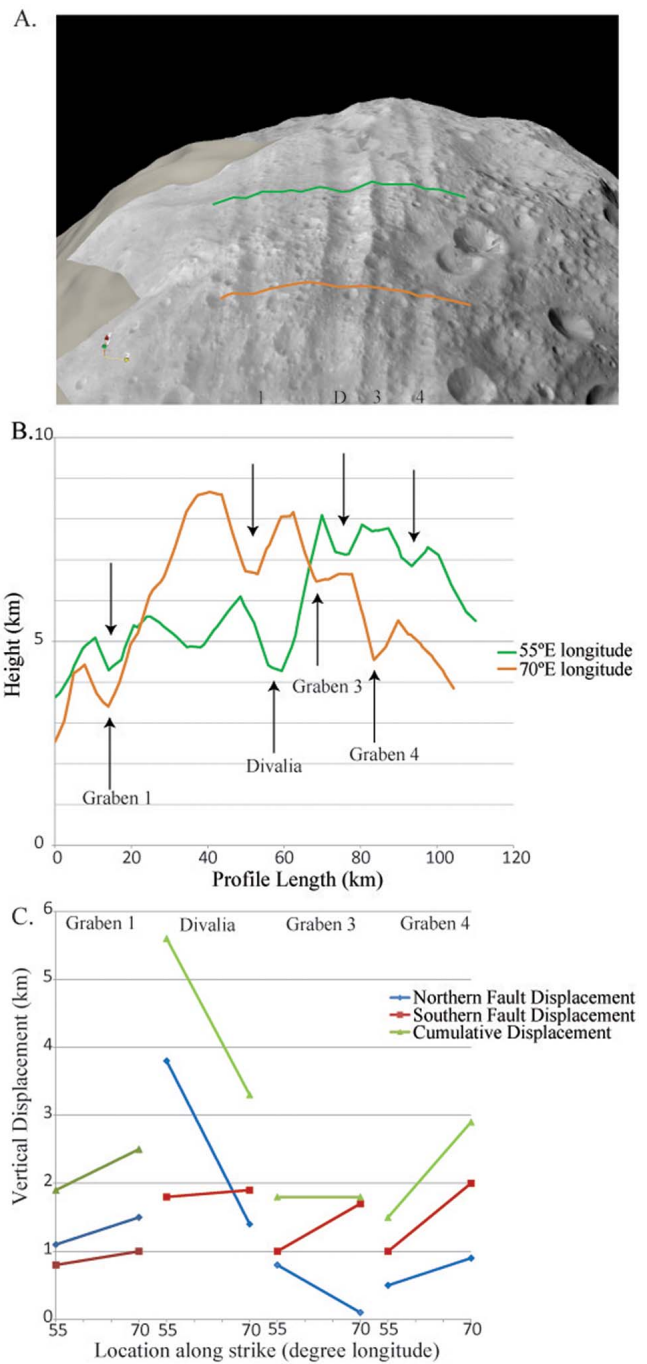


Figure 3. (a) FC images draped over the Vesta shape model in the SBMT shows location of profiles across the troughs. Lines are color-coded to profiles in Figure 3b. (b) Relative topography of four equatorial troughs (including Divalia) at 55°E and 70°E longitude. Profiles go from south to north across the troughs. Vertical exaggeration is $\times 10$. (c) Displacement on the northern (blue) and southern (red) faults of Divalia Fossa and cumulative displacement (green) on the graben are shown for each of the four troughs.

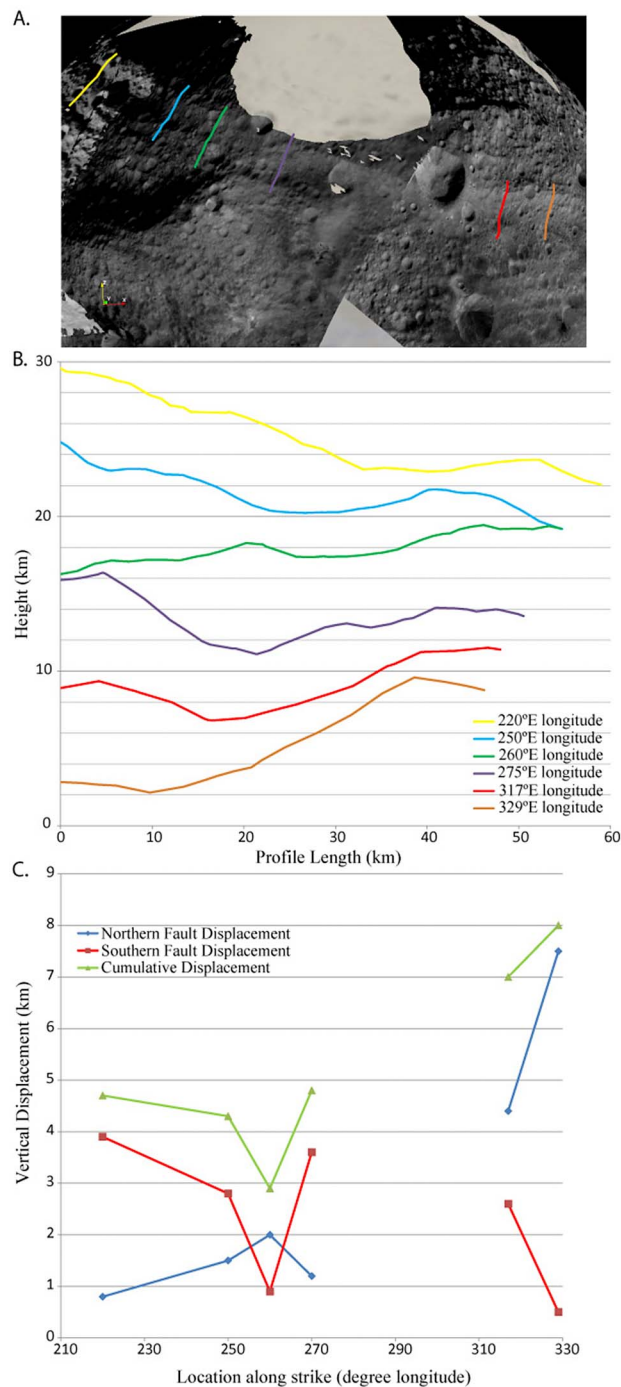


Figure 4. (a) FC images draped over the Vesta shape model in the SBMT shows location of profiles across Saturnalia Fossa. Lines are color-coded to profiles in Figure 4b. (b) Relative topography of Saturnalia Fossa at 220°E, 250°, 260°E, 275°E, 317°E, and 329°E longitude. Profiles go from southwest to northeast across the trough. Vertical exaggeration is $\times 2$. (c) Displacement on the northern (blue) and southern (red) faults of Divalia Fossa and cumulative displacement (green) on the graben.

2.2. Saturnalia Fossa and the Northern Troughs

[8] A second set of linear structures extend to the northwest from the equatorial troughs (Figure 1b). The primary structure in this group is named Saturnalia Fossa (Figure 1b).

Starting at Lepida crater (Figure 1b), Saturnalia is up to 39.2 km wide and extends north for 366 km, into the north polar region that the FC has not yet imaged. In the region north of Vestalia Terra, there are smaller graben and grooves ranging from 31–212 km long that are parallel to Saturnalia (Figure 1b). We have mapped 7 linear structures with this orientation.

[9] Saturnalia Fossa has generally shallower walls than Divalia, with rounded edges and infilling on the trough floor. Both the trough walls and floor appear to have heavier cratering than the equatorial troughs, although this has not yet been quantitatively shown. This all suggests that Saturnalia is older than Divalia and the other equatorial structures, and is consistent with the fault plane analysis that ties its formation to Veneneia basin [Jaumann *et al.*, 2012]. Despite the erosion and infilling, the trough floor is generally flat (or rounded where erosion is most extensive), indicating that it is a graben along its length (Figure 4a). Although both of Saturnalia's scarp faces are heavily eroded and cratered, the southern scarp is generally higher and steeper than the northern scarp (Figure 4a). Analysis of the Saturnalia Fossa profiles indicate the graben accommodates at least 4 km of vertical displacement (Figure 4b), with the southern fault accommodating the bulk of the strain.

[10] To the south of Lepida crater is a 35.4 km wide graben that extends approximately 108 km southeast, ending where it meets the equatorial troughs at $\sim 345^\circ\text{E}$. This southern graben has a higher and steeper northern scarp and profiles suggest that it is a half-graben (Figure 4a). Vertical displacement is between 7 and 8 km. Despite these differences from the northern graben, we propose that this southern feature is a continuation of Saturnalia Fossa. Although the crater eliminates all evidence of connection between the northern or southern fault scarps, a fault plane analysis similar to those performed on Eros [Buczowski *et al.*, 2008] or previously on Vesta [Jaumann *et al.*, 2012] shows that these two graben are co-planar, supporting the interpretation that they were once a single feature. If true, this would mean that Saturnalia Fossa is in fact 552 km long, approximately 33% of Vesta's circumference.

3. Discussion

3.1. Fault Displacement Analysis

[11] In terrestrial graben formation, the magnitude of the displacement is often controlled by a dominant fault, but that dominance can flip back and forth along strike [Blair and McPherson, 1994]. In low sedimentary environments, displacement along the more active fault causes the graben floor to be tilted toward that fault [Blair and McPherson, 1994]. As strain is partitioned to the other fault, graben floor orientation shifts as well. Graben floors in both Divalia and Saturnalia Fossae show similar relationships of graben floor tilt toward the dominant fault. Furthermore, long faults can be comprised of many smaller faults of similar orientation that have linked together. A series of linked faults – some hard linked, some just overlapping fault tips that haven't broken through – could be expressed at the surface as one long continuous graben [Ferrill *et al.*, 1999; Wyrick *et al.*, 2011].

[12] Displacement profiles, charts of the displacement versus length relationship of faults, have been used on Earth [e.g., Cartwright *et al.*, 1995] and other planets [e.g., Schultz

et al., 2006; *Wyrick et al.*, 2011] to describe and interpret the evolution of faults on terrestrial bodies. Our analysis of the displacement profiles across Divalia and Saturnalia Fossae indicates that these graben aren't necessarily a single long continuous fault. The southern Divalia fault effectively tips to zero displacement at $\sim 20^\circ\text{E}$ (Figure 2b), then increases again. This suggests that the southern Divalia fault is comprised of at least two large linking faults, with linkage occurring $\sim 20^\circ\text{E}$. It is also possible that the dip in displacement along the northern Divalia fault at 70°E (Figure 2b) represents the linkage site of two faults comprising the northern bounding fault. Similarly, the small dip in displacement on the Saturnalia southern fault at 260°E (Figure 4b) might suggest that two faults link at this location; strain was instead primarily accommodated at the northern fault here. Meanwhile, the large vertical displacement on the graben south of Lepida crater suggests that these faults were reactivated, perhaps by the event that formed the equatorial troughs.

3.2. Modeling and Implications

[13] Linear structures have been identified on several asteroids in a concentric orientation around impact craters. Grooves were identified on the asteroid Ida around the Vienna Regio concavity [*Asphaug et al.*, 1996], but they did not appear to be features that resulted from large displacements. Linear structures were similarly identified around the Himeros crater on the asteroid Eros [*Prockter et al.*, 2002; *Buczowski et al.*, 2008], but the Eros topographic data reveals that the majority were grooves and fractures with a v-shaped morphology [*Buczowski et al.*, 2008] completely different from the squared-off or U-shaped morphology of the Vesta troughs (Figures 2–4). The few flat-floor troughs concentric to Himeros are considerably shallower than the Vesta troughs and the amount of vertical displacement accommodated is considerably smaller, especially when scaled to the relatively narrow width of the Eros features [*Buczowski et al.*, 2008]. A set of lineaments more than 50 km long and up to 1.2 km wide on Lutetia are nearly concentric to the North Polar Crater Cluster [*Thomas et al.*, 2012]. Topographic data (60 m/pixel raster DTM) of Lutetia indicates that the grooves are shallow (<50 m deep) [*Preusker et al.*, 2012b] and they appear geomorphically similar to the troughs on Eros. While Vesta's equatorial and northern troughs are in a similar orientation around a basin [*Jaumann et al.*, 2012], their geomorphology and displacement profiles are far more like planetary faults than they are like the features on Ida, Eros and Lutetia. Although the fault plane analysis [*Jaumann et al.*, 2012] implies that impact may have been responsible for triggering the formation of these features as on the other asteroids, the morphological and structural differences in the resulting features implies that there must be inherent differences between Vesta and the other asteroids.

[14] This difference could be as simple as asteroid composition. Both spectroscopic studies of Vesta [e.g., *McCord et al.*, 1970; *Gaffey*, 1997] and laboratory studies of HED meteorites (long thought to be Vesta samples) [e.g., *Drake*, 1979] have suggested that there might be a diversity of rock types on Vesta; recent analysis of Dawn data have supported these previous studies [e.g., *DeSanctis et al.*, 2012; *Reddy et al.*, 2012]. In contrast, Ida [*Sullivan et al.*, 1996] and Eros [e.g., *Trombka et al.*, 2000] are both compositionally homogeneous. Vesta may behave more akin to planetary

bodies that have mechanical stratigraphy, alternating layers of mechanically strong and weak rock. The mechanical contrasts of a layered stratigraphy allow for larger scale features, such as graben, to form. Therefore it is possible that graben formed on Vesta and not the other asteroids simply because Vesta is comprised of multiple layers of differing rock types and strengths.

[15] Other possibilities are related to the fact that Vesta is a differentiated body with a mantle and core [*Russell et al.*, 2012]. When stress builds up in rocks it is dissipated by the release of strain, but how strain is released depends on the rheology of the rock. Ductile rocks, such as mantle material, accumulate deformation gradually. Meanwhile, brittle crustal rocks undergo instantaneous stress release and fracture. However, a fault in ductile rocks can also release instantaneously when the strain rate is too great. It is not unlikely that the strain rate due to giant impact on Vesta would be large enough to result in the instantaneous release of strain in its ductile interior, with concurrent large-scale brittle strain on the surface of the asteroid.

[16] The differentiated interior could also be responsible for the formation of graben on Vesta by amplifying and reorienting the stresses resultant from impact, as compared to impact on an undifferentiated body. Preliminary CTH hydrocode [*McGlaun et al.*, 1990] models of a 530 km sphere composed of a basalt analog with a 220 km iron core [*Russell et al.*, 2012] show that the impact of a 50 km object results in different patterns of tensile stress and pressure compared to an undifferentiated sphere of the same material and diameter. While these first-order models have yet to fully mimic the observations made on Vesta, they do demonstrate that the density contrast in Vesta's differentiated interior affects the stresses resulting from the Rheasilvia and Veneneia impacts. It is this impedance mismatch that we suggest is responsible for the development of Vesta's planet-like troughs. On the other hand, impact stresses unaffected by a core would more likely yield the fractures and smaller flat-floored troughs observed on undifferentiated asteroids such as Eros and Ida. Although Lutetia is partially differentiated [*Sierks et al.*, 2011b] it does not display features on the scale of Vesta's troughs, quite possibly because it does not have a fully differentiated core and thus there is a lower density contrast.

4. Conclusions

[17] We have evaluated the morphology of the large-scale structures on Vesta and found that the length, width, depth and shape of these features suggest that they are fault-bounded graben. Their vertical displacement versus length relationship was evaluated and the evolution of the component faults interpreted and described. Although their orientation implies that their formation is tied to the impact events that formed the Rheasilvia and Veneneia basins, features that form due to impact on smaller asteroids are fractures or grooves, not graben. We show that it possible that Vesta's differentiated interior is responsible for the differences in how this impact-related fracturing is expressed.

[18] **Acknowledgments.** The authors gratefully acknowledge the Framing Camera team, as well as the support of the Dawn Science, Operations and other Instrument Teams. This research is supported by the National Aeronautics and Space Administration under grant NNX10AR58G issued through the Science Mission Directorate Dawn at Vesta Participating Science Program.

[19] The Editor thanks Robert Anderson and Geoffrey Collins for assisting in the evaluation of this paper.

References

- Asphaug, E., J. M. Moore, D. Morrison, W. Benz, M. C. Nolan, and R. J. Sullivan (1996), Mechanical and geological effects of impact cratering on Ida, *Icarus*, *120*, 158–184, doi:10.1006/icar.1996.0043.
- Blair, T. C., and J. G. McPherson (1994), Historical adjustments by Walker River to lake-level fall over a tectonically tilted half-graben floor, Walker Lake Basin, Nevada, *Sediment. Geol.*, *92*(1–2), 7–16, doi:10.1016/0037-0738(94)00058-1.
- Buczkowski, D. L., O. S. Barnouin, and L. M. Prockter (2008), 433 Eros lineaments: Global mapping and analysis, *Icarus*, *193*, 39–52, doi:10.1016/j.icarus.2007.06.028.
- Buczkowski, D. L., et al. (2012), Geologic mapping of the Av-9 Numisia Quadrangle of asteroid 4 Vesta, *Lunar Planet. Sci. Conf.*, *43rd*, Abstract 2263.
- Cartwright, J. A., B. D. Trudgill, and C. S. Mansfield (1995), Fault growth by segment linkage: An explanation for scatter in maximum displacement and trace length data from the Canyonlands Grabens of SE Utah, *J. Struct. Geol.*, *17*, 1319–1326, doi:10.1016/0191-8141(95)00033-A.
- DeSantis, M. C., et al. (2012), Overview of Vesta mineralogy diversity, *43rd Lunar Planet. Sci. Conf.*, Abs. 1444, Houston TX.
- Drake, M. J. (1979), Geochemical evolution of the eucrite parent body: Possible evolution of asteroid 4 Vesta?, in *Asteroids*, edited by T. Gehrels and M. S. Matthews, pp. 765–782, Univ. of Ariz. Press, Tucson.
- Ferrill, D. A., J. A. Stamatakos, and D. Sims (1999), Normal fault corrugation: Implications for growth and seismicity of active normal faults, *J. Struct. Geol.*, *21*(8–9), 1027–1038, doi:10.1016/S0191-8141(99)00017-6.
- Gaffey, M. J. (1997), Surface lithologic heterogeneity of asteroid 4 Vesta, *Icarus*, *127*, 130–157, doi:10.1006/icar.1997.5680.
- Gibbs, A. D. (1987), Deep seismic profiles in the northern North Sea, in *Petroleum Geology of the North West Europe*, edited by J. Brooks and K. Glennie, pp. 1025–1028, Graham and Trotman, London.
- Jaumann, R., et al. (2012), Vesta’s shape and morphology, *Science*, *336*, 687–690, doi:10.1126/science.1219122.
- Kahn, E. G., O. S. Barnouin, D. L. Buczkowski, C. M. Ernst, N. Izenberg, S. Murchie, and L. M. Prockter (2011), A tool for the visualization of small body data, *Lunar Planet. Sci. Conf.*, *42nd*, Abstract 1618.
- McCord, T. B., J. B. Adams, and T. V. Johnson (1970), Asteroid Vesta: Spectral reflectivity and compositional implications, *Science*, *168*, 1445–1447, doi:10.1126/science.168.3938.1445.
- McGlaun, J. M., S. L. Thompson, and M. G. Elrick (1990), CTH: A three-dimensional shock wave physics code, *Int. J. Impact Eng.*, *10*, 351–360, doi:10.1016/0734-743X(90)90071-3.
- Preusker, F., F. Scholten, K.-D. Matz, R. Jaumann, T. Roatsch, C. A. Raymond, and C. T. Russell (2012a), Topography of Vesta from Dawn FD stereo images, *Lunar Planet. Sci. Conf.*, *43rd*, Abstract 2012.
- Preusker, F., F. Scholten, J. Knollenberg, E. Kuhr, K.-D. Matz, S. Mottola, T. Roatsch, and N. Thomas (2012b), The northern hemisphere of asteroid (21) Lutetia—Topography and orthoimages from Rosetta OSIRISNAC image data, *Planet. Space Sci.*, *66*, 54–63, doi:10.1016/j.pss.2012.01.008.
- Prockter, L., P. Thomas, M. Robinson, J. Joseph, A. Milne, B. Bussey, J. Veverka, and A. Cheng (2002), Surface expressions of structural features on Eros, *Icarus*, *155*, 75–93, doi:10.1006/icar.2001.6770.
- Reddy, V., et al. (2012), Albedo and color heterogeneity of Vesta from Dawn, *Science*, *336*, 700–704, doi:10.1126/science.1219088.
- Russell, C. T., and C. A. Raymond (2011), The Dawn mission to Vesta and Ceres, *Space Sci. Rev.*, *163*, 3–23, doi:10.1007/s11214-011-9836-2.
- Russell, C., et al. (2012), Dawn at Vesta: Testing the paradigm, *Science*, *336*, 684–686, doi:10.1126/science.1219381.
- Schultz, R. A., C. H. Okubo, and S. J. Wilkins (2006), Displacement-length scaling relations for faults on the terrestrial planets, *J. Struct. Geol.*, *28*, 2182–2193, doi:10.1016/j.jsg.2006.03.034.
- Sierks, H., et al. (2011a), The Dawn Framing Camera, *Space Sci. Rev.*, *163*, 263–327, doi:10.1007/s11214-011-9745-4.
- Sierks, H., et al. (2011b), Images of Asteroid 21 Lutetia: A remnant planetesimal from the early solar system, *Science*, *334*, 487–490, doi:10.1126/science.1207325.
- Sullivan, R., et al. (1996), The geology of 243 Ida, *Icarus*, *120*, 119–139, doi:10.1006/icar.1996.0041.
- Thomas, N., et al. (2012), The geomorphology of (21) Lutetia: Results from the OSIRIS imaging system onboard ESA’s Rosetta spacecraft, *Planet. Space Sci.*, *66*, 96–124, doi:10.1016/j.pss.2011.10.003.
- Trombka, J. I., et al. (2000), The elemental composition of asteroid 433 Eros: Results of the NEAR-Shoemaker X-ray Spectrometer, *Science*, *289*, 2101–2105, doi:10.1126/science.289.5487.2101.
- Wyrick, D. Y., A. P. Morris, and D. A. Ferrill (2011), Normal fault growth in analog models and on Mars, *Icarus*, *212*, 559–567, doi:10.1016/j.icarus.2011.01.011.